International Journal of Engineering and Advanced Technology (IJEAT)
ISSN: 2249-8958 (Online), Volume-9 Issue-2, December, 2019

# Medical Image Compression by Optimal Filter Coefficients Aided Transforms using Modified Rider Optimization Algorithm

**P .Sreenivasulu, S. Varadha Rajan, S. Thenappan**

***ABSTRACT---Owing to a large amount of images, image compression is requisite for minimizing the redundancies in image, and it offers efficient transmission and archiving of images. This paper presents a novel medical image compression model using intelligent techniques. The adopted medical image compression comprises of three major steps such as, Segmentation, Image compression, and Image decompression. Initially, the Region of Interest (ROI) and Non-ROI regions of the image are split by means of a Segmentation procedure using Modified Region Growing (MRG) algorithm. Moreover, the image compression process begins which is varied for both ROI and Non-ROI regions. On considering the ROI regions, the compression is carried out by Discrete Cosine Transform (DCT) model and SPIHT encoding method, whereas the compression of Non-ROI region is carried out by Discrete Wavelet Transform (DWT) and Merge-based Huffman encoding (MHE) methods. As a main contribution, this paper intends to deploy the optimized filter coefficients in both DCT and DWT techniques. Here, the optimization of both filter coefficients is performed using Modified Rider Optimization Algorithm (ROA) called Improvised Steering angle and Gear-based ROA (ISG-ROA). In the final step, decompression is done by implementing the reverse concept of compression process with similar optimized coefficients. The filter coefficients are tuned in such a way that the Compression Ratio (CR) should be minimum. In addition, the comparative analysis over the state-of-the-art models proves the superior performance of the proposed model.***

***Keywords— Image compression; Region of Interest; Discrete Cosine Transform, Discrete Wavelet Transform, Filter Coefficients; Modified Rider Optimization Algorithm***

**Nomenclature**

| Acronyms | Descriptions |
|---|---|
| ROI | Region Of Interest |
| MRI | Magnetic Resonance Imaging |
| CT | Computed Tomography |
| US | Ultrasound |
| PET | Positron Emission Tomography |
| ECG | Electrocardiogram |
| LIS | List of Insignificant Sets. |
| LIP | List of Insignificant Pixels. |
| LSP | List of Significant Pixels. |
| IWT | Integer Wavelet Transform |
| LHT | Lossless HadamardTransformation |
| NTB | Non-Transformed Block |
| CR | Compression Ratio |
| 3D | Three-Dimensional |
| SPIHT | Set Partitioning In Hierarchical Trees |
| SBD | Separate Descendant-Based |
| FF | FireFly |
| PSO | Particle Swarm Optimization |
| GWO | Grey Wolf Optimization |
| WOA | Whale Optimization Algorithm |
| ROA | Rider Optimization Algorithm |
| HEVC | High Efficiency Video Coding |
| MRPs | Minimum Rate Predictors |
| US | UltraSound |
| GRE | Golomb–Rice Encoder |
| DCT | Discrete Cosine Transform |
| ISG-ROA | Improvised Steering angle and Gear-based ROA |
| DWT | Discrete Wavelet Transform |
| 2D | Two-Dimensional |
| AFB | Analysis Filter Bank |
| LPF | Low Pass Filters |
| MEP | Mean Error Percentage |
| HPF | High Pass Filters |
| MEP | Mean Error Percentage |
| SMAPE | Symmetric Mean Absolute Percentage Error |
| MASE | Mean Absolute Scaled Error |
| MAE | Mean Absolute Scaled Error |
| RMSE | Root Mean Square Error |
| TP | True Positive |
| TN | True Negative |
| FPR | False Positive Rate |
| FNR | False Negative Rate |
| NPV | Net Present Value |
| FDR | False Discovery Rate |
| MCC | Matthew's Correlation Coefficient |

## I. INTRODUCTION

Image compression [1] [2] [3] is the process of reducing the size of bytes in a graphics file devoid of deteriorating the image quality to an undesirable level. The minimization in file size permits more images to be stored in a specified memory space or disk. It moreover minimizes the time duration for images to be transmitted over the Internet or downloaded from Web pages [4] [5] [6]. There exist numerous varied methods by which the image files could be compressed. The two most general compressed graphic image formats for internet use are the GIF format and the JPEG format. Image compression approaches could be generally categorized into two models, (a) Lossy Image Compression (b) Lossless Image Compression. Lossless image compression techniques do not cause any data loss.

Revised Manuscript Received on December 30, 2019.

* Correspondence Author

**P .Sreenivasulu,** Research Scholar, ECE Department, Sri Venkateswara University College of Engineering, Titupati, A.P, India. Email: sreenu306@gmail.com

**Dr. S. Varadha Rajan,** Professor, Dept Of ECE, S V University, Tirupati, Email: varadasouri@gmail.com

**Dr. S. Thenappan,** Professor,ECE, Dept Of ECE, KNSIT ,Banglore, Karnataka, India.. Email: honey.souri@gmail.com

Different from lossless image compression, lossy image compression models causedata loss and therefore experience a loss of quality in restoration[7] [8] [9]. Medical images [10] [11] comprise of enormous quantity of data that assist doctors to examine the data effectively, and it further helps in treating the patients. Storing these medical images [12] [13] remains a critical task for the hospital owing to the storage needs. These images are accumulated in digital form that is simpler to examine. To beat the issue of picture stockpiling, pressure process is vital. Inferable from pressure, pictures [14] [15] lose their information that causes risk all through conclusion or treatment; in this way it prompts to display a capable methodology for recreation and pressure to moderate the nature of picture with diminished transmission time. Treating the sicknesses utilizing restorative pictures [16] [17] has achieved a much huge spot these days, notwithstanding; it devours more data transmission. For telemedicine machines, these medicinal pictures [18] [19] must to be transmitted to different goals. Therapeutic pictures in particular, MRI, CT, US, PET, and ECG require to be put away and transmitted for confirming by another restorative authority whenever required. These huge amounts of data cause a colossal measure of memory usage, and it raises the traffic and time all through transmission. In this manner, medicinal picture pressure [20] is important to limit the data transfer capacity and capacity prerequisites. Various profoundly created restorative picture pressure systems [21] [22] were executed for medicinal pictures because of the rising requests. JPEG is a propelled picture pressure apparatus, yet, it requires picture level access and couldn't destroy the relationship inside the sub groups. Most essentially, these are lossy methodologies and couldn't be capable for restorative pictures  This paper contributes a propelled medicinal picture pressure model through a few procedures like Segmentation, Image pressure, and Image decompression. Here, from the outset, the ROI and Non-ROI segments of the picture are partitioned utilizing MRG model. The pressure in ROI areas is finished utilizing DCT and SPIHT encoding strategy, while, the pressure of Non-ROI locale is finished utilizing DWT and MHE models. The principle commitment of this paper is to tune or upgrade the channel coefficients of DCT, and DWT, with the expectation of limiting the CR. An altered calculation called ISG-ROA is utilized for upgrading the channel coefficients. Also, decompression is completed by playing out the invert idea of pressure process with same advanced coefficients. The strong approval of the proposed model is finished with the relative examination. The general association of the work is as per the following: Section II depicts the writing work. Area III portrays the medicinal picture pressure: proposed design with division calculation and Section IV clarifies the picture pressure methodology for ROI and non-ROI. Segment V portrays the channel coefficient streamlining by changed ROA, and Section VI examines the exploratory outcomes, and Section VII closes the paper.

## II. LITERATURE REVIEW

### *A. Related works*

In 2018, Sunil *et al.* [1] have suggested a model to attain the reconstruction of medical image by establishing convex-smoothing issues. This was executed by isolating the input image into sub-issues. As per this scheme, the input image was split into sub-issues that were resolved by means ofcompressed sensing technique. Following the attainment of output compressed image, the proposed system focuses on minimizing the computational complexity, reconstruction error and time. In addition, the presented scheme was analyzed with medical images and outcomes were performed with respect to time, reconstruction error, and PSNR.

In 2015, Zuo*et al.* [2] have established a methodology for image compression based on ROI in order to increase the CR. Initially, the image was split into two portions (i) ROI regions and (ii) non-ROI regions. Lossless compression approaches were then deployed to the indicated portions of ROI, and accordingly, other algorithms were exploited to the erstwhile regions of the image. A group of experimentations was modeled to measure the efficiency of the established compression technique. Here, the investigational outcomes indicate that the established system offers better results than other traditional models.

In 2015, Tim *et al.* [3] have systematically examined the scheme that permits for enhancing the performance of JPEG for medical image compression. Here, a recently introduced generic codec structure was presented that supports JPEG format. A comprehensive objective examination of the performance complexity presented by such schemes was also carried out. In addition, an assessment of the accessible approaches was offered that was compared with the traditional schemes. Moreover, a study on the visual performance of the presented scheme was analyzed when deploying the conventional schemes. This tends to offer several strategies on how to compress medical images optimally at a tolerable complexity range.

In 2016, Venugopal*et al.* [4] have adopted a block-based image compression approach by means of Huffman encoding and Hadamard transform that was a trouble-free model with less intricacy. Primarily, input image was disintegrated by IWT and LHT, which was deployed to eradicate the correlation within the block. The major importance of this technique was its effectual truncation and substantiation. Depending on the outcome of NTB, encoding was made directly or subsequent to conversion by LHT model. From the outcomes, it was noticed that the adopted scheme attains improved performances with respect to CR and it was quite efficient when distinguished with conventional models.

In 2017, Haddad *et al.* [5] have suggested a novel joint watermarking-compression method for modulating the watermarking systems. This method permits access to watermarking-depending security services devoid of image decompression. It turns out to be feasible to mark out images or to confirm their accuracy from their compressed bitstream directly. The performance was articulated with respect to distortion and embedding capacity and was estimated on ultrasound images. They demonstrated that watermarked images do not differ from their real counterparts when providing a better ability to support diverse security services. In addition, the implemented scheme was analyzedwith respect to image authenticity and reliability.

In 2017, Song et al. [6] have presented a quick pressure approach for restorative picture successions with high-goals, known as 3D SDB-SPIHT plot.

For accelerating the transformation, 3D whole number wavelet change was misused at first. Contingent upon a capable spatial-transient mode, a quick coding framework was presented by parceling

the descendants set into leaves set and posterity set. The presented plan has greater selectivity in choosing the checking and coding of the relative sets and consequently the coding time is quickened. The test results have demonstrated that the displayed plan offers quicker medicinal picture pressure when contrasted and customary models.

In 2018, Parikh et al. [7] have set up a philosophy based that depicts the use of HEVC for analytic restorative picture pressure, worried on CR. As needs be, lossy pressure plans identified with the therapeutic picture pressure were investigated. Contingent upon a presented worthy pressure level for JPEG, this plan presents good HEVC pressure for a few apparatuses. The investigational results showed that HEVC could raise the CR by 54% and thus, a novel procedure for limiting computational multifaceted nature of HEVC encoding was built up. Results showed that the complexities in HEVC could be limited by over 55% with slight ascent in document size.

In 2017, Lucas *et al.* [8] have introduced a highly competent technique termed as 3-D-MRP, which was depending on the theory of MRPs. The most important characteristics of the established technique compriseof the exploitation of 3-D predictors, classification and3-D-block octree separation and volume dependent optimization. Moreover, investigational outcomes revealed the effectiveness of the established technique for the compression of medical images, that attains about 12% and 15% for 16 and 8bit depth contents, correspondingly, while evaluated with other traditional schemes.

### *B. Review*

Table 1 show the methods, features, and challenges of conventional techniques for the medical image compression. At first, Langragian framework was introduced in [1], which recognizes zero-day attack, and it also offers increased PSNR. However, it needs more time. ROI algorithm was exploited in [2] that offers better efficiency, and it also offers high degree of compression, but it has to focus more on real time applications. In addition, DWT approach was deployed in [3] that provide improved CR, and it also offers better compression efficiency. However, executions were not optimized for computational evaluation. Likewise, LHT scheme was exploited in [4], which offers improved CR, and it also enhances the better band storage. However, it requires contemplation on colour image compression models. Also, GRE model was employed in [5], which guarantees better visual quality and large capacity regarding security services; however it has to focus more on the quality of the image. 3D SDB-SPIHT model was exploited in [6] that provide fast compression, and it minimizes the duration of coding, yet, it has to be deployed to various types of images. HEVC was implemented in [7], which minimizes complexity and it also offers increased file size, but an increase in complexity increases the time. In addition, MRP was suggested in [8] that minimize the time consumption, and it offers reduced complexity. However, it needs consideration on maximum memory utilization. Thence, these limitations have to be considered for improving the performance of medical image compression models effectively in the current research work.

**Table:I Features and challenges of state-of-the-art medical image compression models using various techniques**

| Author [citation] | Adopted methodology | Features | Challenges |
|---|---|---|---|
| Sunil*et al.* [1] | Langragian framework | ❖ Minimizes complexity.<br>❖ Increased PSNR. | ❖ Increased time consumption. |
| Zuo*et al.* [2] | ROI | ❖ Better efficiency<br>❖ High degree of compression | ❖ Requires contemplation on real time applications |
| Tim *et al.* [3] | DWT | ❖ Improved CR<br>❖ Better compression efficiency. | ❖ The executions were not optimized for computational evaluation. |
| Venugopal *et al.* [4] | LHT | ❖ Improved CR<br>❖ Better band effective storage. | ❖ Requires contemplation on colour image compression models. |
| Haddad *et al.* [5] | GRE | ❖ Guarantees better visual quality.<br>❖ Large capacity regarding security services. | ❖ Have to focus more on the quality of the image. |

## III. MEDICAL IMAGE COMPRESSION: PROPOSED ARCHITECTURE WITH SEGMENTATION ALGORITHM

### *A. Architectural Representation*

The diagrammatic portrayal of the proposed medicinal picture pressure model is appeared in Fig. 1. In this exploration work, a novel therapeutic picture pressure model is executed utilizing wise strategy. The proposed restorative picture pressure includes three principle steps in particular, Segmentation, Image pressure, and Image decompression. At first, the ROI and Non-ROI districts of the picture are part utilizing a division procedure known as MRG calculation. After picture division, the sectioned yield is oppressed for picture pressure, which is distinctive for the two ROI and Non-ROI locales. On assessing the ROI locales, the pressure is performed by DCT model and SPIHT encoding technique. Then again, the pressure of Non-ROI locale is performed by DWT and MHE technique. What's more, advancing channel coefficients of both DCT and DWT techniques assumes a significant job in this pressure model, which is considered as the significant commitment. (i.e) the enhancement of both channel coefficients is performed utilizing adjusted ROA approach named as ISG-ROA calculation. After pressure process, decompression is performed via completing the turn around idea of pressure with the equivalent streamlined coefficients.

The target should concentrate on minimization of CR, which totally relies upon the tuning of channel coefficients of both DCT and DWT

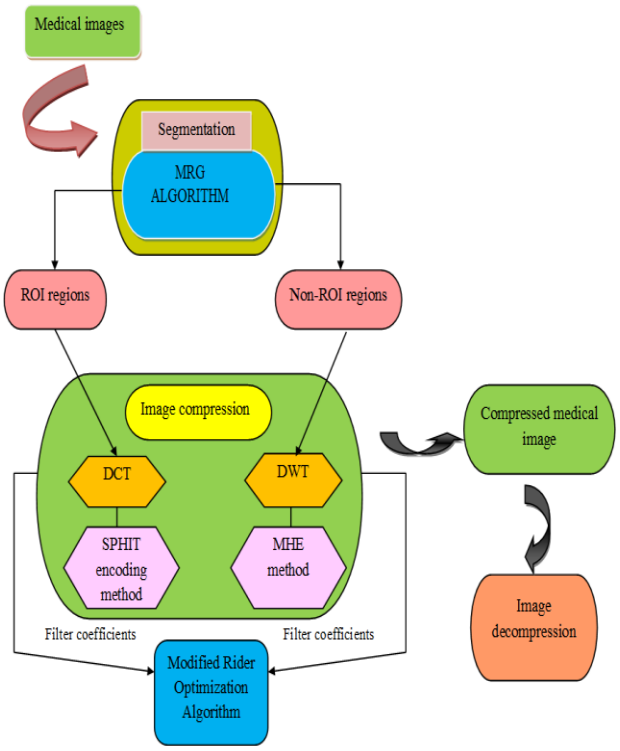


**Fig.1 Diagrammatic representation of the proposed medical image compression model**

*B. Segmentation using Modified Region growing method*

Region growing is a region-based image segmentation model, and it comprises of the assortment of initial seed points [31]. In this work, MRG is deployed for segmenting the ROI regions from the image. Assume that the size of input image, $I(i,j)$ be 256×256. At first, the ROI region of $I(i,j)$ is segmented. Here the segmentation of $I(i,j)$ takes place by means of seed point, which has to be regulated. A seed point is "the beginning stage for district developing and its determination is noteworthy for the division arrangement". The means of the MRG approach are delineated beneath.

Step 1: The input image $I(i,j)$ is split into several blocks $P$, in which every block includes one centre pixel and numerous neighborhood pixels.

Step 2: In the second step, intensity threshold $(R^i)$ is fixed.

Step 3: For all block $P$, perform the following processes till the count of blocks attains the total number of blocks for an image.

Step 3(a): Determine the histogram $G$ of every pixel in $P$ .

Step 3(b): Adjust the most repetitive histogram of the $P^{th}$ block, which is indicated by $U^h$.

Step 3(c): Choose any pixel, based on $U^h$ and assign a pixel as seed point with intensity $Int_u$ .

Step 3(d): Deliberate the adjacent pixel having the intensity, $Int_n$ .

Step 3(e): - Determine the intensity difference of those pixels $u$ and $n$ .(i.e.) $Dif_{Int} = \|Int_u - Int_n\|$

Step 3(f): If $Dif_{Int} < R^i$ , sum up the consistent pixel to the region, and thus the region will be grown, or follow step 3(h).

Step 3(g): Verify if the entire pixels are summed up to the region. If yes, follow step 2 and then follow step 3(h).

Step 3(h): Re-estimate the region and identify the novel seed points and carry out the process from step 3(a).

Step 4: - End the total process.

Thus the ROI and Non ROI regions obtained after segmentation using MRG algorithm are denoted by $I_{ROI}$ and $I_{NROI}$ .

## IV. IMAGE COMPRESSION PROCEDURE FOR ROI AND NON-ROI

The ROI regions of the image are compressed using DCT and SPIHT encoding method, while the Non-ROI regions of the image are compressed using DWT and MHE methods.

*A. Discrete Cosine Transform*

The ROI region of the medical image is initially given to DCT. In general, DCT [29] is a major concept in image processing domain, and it has the better capability of information centralizing for images source. Thus, it is renowned for its advanced performances of simple execution and energy compaction. Eq. (1) describes the 2D DCT of a block of image $N \times N$ .

$$F(q,v) = \frac{2}{N} d(q)d(v) \sum_{i=0}^{N-1} \sum_{j=0}^{N-1} f(i,j) \cos\left(\frac{\pi(2i+1)q}{2N}\right) \cos\left(\frac{\pi(2j+1)q}{2N}\right), q,v = 0,1,2...N-1 \quad (1)$$

$$f(q,v) = \frac{2}{N} \sum_{i=0}^{N-1} \sum_{j=0}^{N-1} d(q)d(v)F(i,j) \cos\left(\frac{\pi(2i+1)q}{2N}\right) \cos\left(\frac{\pi(2j+1)q}{2N}\right), q,v = 0,1,2...N-1 \quad (2)$$

In Eq. (2), $f(q,v)$ indicates $(q,v)^{th}$ image pixel value present in spatial domain, and $F(q,v)$, indicates $(q,v)^{th}$ DCT coefficient in frequency domain; $d(k)$ indicates multiplication parameter as shown in Eq. (3).

$$d(k) = \begin{cases} \frac{1}{\sqrt{2}}, & if \quad k = 0 \\ 1, & if \quad k > 0 \end{cases} \quad (3)$$

*B. SPIHT encoding method*

The DCT output is subjected to SPIHT encoding model. In SPIHT encoding scheme [30], the wavelet coefficients are indicated by tree structure. SPIHT scheme is portrayed as given below.

The significance test $O_n(T)$ on concerning the wavelet coefficients is given by Eq. (4), where $g_{i,j}$ indicatescoefficient of $(i,j)$node, $T$ denotes testing set.

$$O_n(T)=\begin{cases}1, & \max\limits_{(i,j)\in T}\left\{\left|g_{i,j}\right|\right\}\geq 2^n \\ 0, & otherwise\end{cases} \quad (4)$$

The coding techniqueis portrayed by the below steps.

**Step 1:Initialization**.

Evaluate $n=\left\lfloor \log_2\left(\max\limits_{(i,j)\in T}\left\{\left|g_{i,j}\right|\right\}\right)\right\rfloor$, fix LSP equivalent to zero, shift the entire top nodes $(i,j)$to LIP, and shift those with successorsto LIS, whenremarking $A$ type.

**Step 2: Sorting**.

1. For every node $(i,j)$ of LIP: Evaluate $O_n(i,j)$;

2. If $O_n(i,j)=1$, shift node $(i,j)$to LSP and yield the symbolof $g_{i,j}$.

For every node $(i,j)$of LIS:

1. If nodeis belonged to $A$ type,

(a) Evaluate $O_n(H(i,j))$;

(b) If $O_n(H(i,j))=1$, for entire nodes $(k,l)$of $S(i,j)$, output $O_n(k,l)$:

- if $O_n(k,l)=1$, shift node $(k,l)$to LSP and yield the symbol of $g_{k,l}$, l;
- if $O_n(k,l)=0$, shift node $(k,l)$to LIP.

(c) if $l(i,j)$is not vacant, shift node $(i,j)$to the lower portion of LIS as $B$ type and shift to (3); or else, discard node $(i,j)$from LIS.

2. If nodeis belonged to $B$ type,

(a) Evaluate $O_n(l(i,j))$;

(b) If $O_n(l(i,j))=1$, shiftevery node of $S(i,j)$to LIS as $A$ typeand discard node $(i,j)$from LIS.

**Step 3: Refinement sorting.** For entire nodes $(i,j)$of LSP, other than those come to view in the final sorting process, yield the $nth$ bit value of $\left|g_{i,j}\right|$.

**Step 4: Quantization updating.** If $n=0$, terminate; or, reduce $n$ by one and follow Step 2.

Thus the attained image compressed ROI regions using DCT and SPIHT encoding methods is indicated by $IC_{ROI}$.

*C. Discrete Wavelet Transform*

The non-ROI regions of therapeutic picture are given to DWT [25] [26] [27], in which the preparing of a picture could be done by transmitting it by means of an AFB following the pulverization work [28]. This AFB contains LPF and HPF that are sent for picture pressure. On transmitting a picture through AFB, it is apportioned into two groups. The HPF achieves the point by point information of the picture. The LPF that is associated to an averaging capacity achieves the entire picture information. The yield of sifting capacities is demolished by two. Also, the mother wavelet is clarified as demonstrated in Eq. (5), in which means move coefficient and alludes to the scale coefficient.

The recent premise tasks are viewed as the mother wavelet separations. $\tau_{m,q}(l)=\frac{1}{\sqrt{m}}\tau\left(\frac{a-q}{m}\right)$ (5)

In 2D DWT, a 2D scaling function, $\varphi(a,b)$and three 2D wavelets, $\tau^H(a,b),\tau^V(a,b)$and $\tau^D(x,y)$are needed. Every component is a product of 1D scaling function $\varphi$ and its respectivewavelet $\tau$. Apart fromthe products, which produce1Doutcomes like $\tau(a)$ and $\varphi(a)$, the remaining fourproducts generate the independent scaling function as specified by Eq. (6) and independent, directional sensitive wavelets as denoted by Eq. (7), Eq. (8) and Eq. (9).

$$\varphi(a,b)=\varphi(a)\varphi(b) \quad (6)$$

$$\tau^H(a,b)=\varphi(a)\tau(b) \quad (7)$$

$$\tau^V(a,b)=\tau(a)\varphi(b) \quad (8)$$

$$\tau^D(a,b)=\tau(a)\tau(b) \quad (9)$$

These wavelets calculate gray level deviations, functional differences or intensity for images, in diverse directions. $\tau^H$ computes the differences along horizontal columns or edges, $\tau^V$ is associated to variations along vertical edges or rows, and $\tau^D$ is associated to variations along diagonals. Translated and scaled basis functions are illustrated as specified in Eq. (10) and Eq. (11), in which, index '$i$' recognizes the directional wavelets and'$j$' indicates the scaling function.

$$\varphi_{j,w,w}(a,b)=2^{\frac{j}{2}}\varphi\left(2^j a-w,2^j y-w\right) \quad (10)$$

$$\tau^i_{j,w,w}(a,b)=2^{\frac{j}{2}}\tau^i\left(2^j a-w,2^j y-w\right), i=\{H,V,D\} \quad (11)$$

Here, a wavelet $W(\tilde{F})$ as given in Eq. (12) is convolved with input image, where $P_k$ refers to the filter coefficient of DWT.

$$W(\tilde{F})=\sum_k P_k\Phi\left(2\tilde{F}-\bar{k}\right) \quad (12)$$

DWT of image $g(a,b)$with size $M\times M$ can be evaluated as provided in Eq. (13) and Eq. (14).

$$\tau_\varphi(j_0,w,w)=\frac{1}{\sqrt{MM}}\sum_{l=0}^{M-1}\sum_{f=0}^{M-1}g(a,b)\varphi_{j_0,w,w}(a,b) \quad (13)$$

$$\tau^i_\tau(j,w,w)=\frac{1}{\sqrt{MM}}\sum_{l=0}^{M-1}\sum_{f=0}^{M-1}g(a,b)\tau^i{}_{j,w,w}(a,b) \quad (14)$$

*D. Merging-based Huffman Encoding (MHE)*

The non-ROI areas of restorative picture are then packed by sending the MHE approach after DCT. MHE plot includes three significant stages:

(I) Formation of Huffman code utilizing unique information.

(ii) Code change subordinate molding and

(iii) Encoding.

*(i) Formation of Huffman code using original data*

- Organize the symbols probabilities in descending order.
- By exploiting the symbols of two smallest probabilities $p_A$ and $p_B$, produce a novel hub, where these two probabilities are branches. Here, the novel hub is marked with the numerical expansion of these two probabilities.
- Proceed with this procedure by conveying the novel code instead of the first two, till just a single hub is left.
- Mark each upper branch with '0' and lower individual from each pair with '1' and the other way around.
- The code of all original symbols is further depicted by starting from the root of the tree to the needed leaf, and accordingly, the branch label of every node is traversed.

*(ii) Code transformation dependent conditioning*

The code transformation of condition-dependent sequence is made prior to the production of Huffman code for every original data or sign. The procedure of code transformation is as follows: At first, the original data with the codewordare obtained. Subsequently, the code transformation is performed by combining the two symbols. Further, the merging procedure is dependent on the below observations:

- Initially, the process of merging is deployed on the chosen symbols that gratifies the condition, (>1 or higher than 1), then, it is qualified for the merging procedure.
- In the second step, the pair, which has the similar amalgamation of the first digit of the chosen pair, should not be repeated.
- In the third step, the bit length of initial position of the pair has to be smaller than the bit length of the 2nd position of pair.
- If the abovementioned three cases are gratified, the 1st position of the sign is recurred two times, and a new pair is substituted in place of older pair or chosen pair.
- Likewise, the abovementioned procedure is recurred for the entire chosen code words.

*(iii) Encoding*

The process of encoding is made depending on the amalgamation of the sign deployed in the code transformation of merging dependent sequence and the previous sign in the original data. The encoding procedure is mentioned below: Initially, the mixture of the signs deployed for the code transformation procedure and the previous sign of the mixture of the symbols used for the code conversion procedure is verified to choose whether the code generated using code transformation procedure is to be regarded or not. Subsequently, above 3 steps are deployed, and every sign are verified for encoding the original data. Followed by this confirmation, a codeis created for the original data. The last code is the encoded data depending on MHE method. Thus the attained image compressed $I_{NROI}$ using DWT and MHE encoding methods is indicated by $IC_{NROI}$ .

## V. FILTER COEFFICIENT OPTIMIZATION BY MODIFIED RIDER OPTIMIZATION ALGORITHM

*A. Objective Function and Solution Encoding*

In the proposed medical image compression model, the major objective function is to minimize the CR of the compressed image as shown by Eq. (16).

$$CR = \frac{Size\ of\ \ compressed\ image}{Size\ of\ \ original\ \ image} = \frac{Size\ of\ \ (I_{ROI} + I_{NROI})}{Size\ of\ \ (IC_{ROI} + IC_{NROI})} \quad (15)$$

$$Objective\ \ function = Min(CR) \quad (16)$$

Accordingly, the filter coefficients of DCT, i.e. $F$ ranging from $F_1$ to $F_{N_F}$, and filter coefficients of DWT, i.e. $P$ ranging from $P_1$ to $P_{N_P}$, is given as input for solution encoding as specified by Fig. 2, where $N_F$ indicates the number of DCT filter coefficients of DCT and $N_P$ indicates the number of DWT filter coefficients.

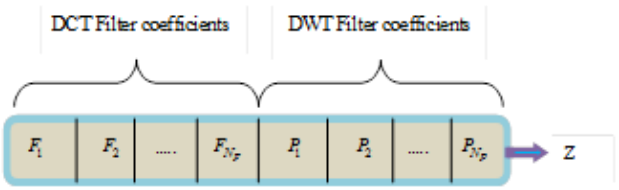


**Fig.2 Solution encoding**

*B. Rider Optimization Algorithm*

The filter coefficients, and of DCT and DWT are given to ROA calculation for improvement. The ROA [24] depends on anecdotal registering that manages the improvement goals by means of the nonexistent hypotheses and thoughts. For the most part, ROA depends on the bunch of Riders that moves towards the comparable goal to be the victor of the race. The stunning thought concerning ROA is in regards to the improved presentation of ROA with diminished advancement time and in like manner performing unrivaled than the other fake processing and nature-propelled enhancements.

**Initialization:** The rider's position is initialized as specified by Eq. (17), in which, $Y$ and $X$ refers to the count of total co-ordinates and riders. $Z^{\tau}(u,h)$ point out the position of $u^{th}$ riderat $\tau$. A total of $B$, $F$, $G$ and $A$ riders, namely, bypass, followers, over takers, and attackers are taken into account in this work.

$$Z^{\tau} = \left\{ Z^{\tau}(u,h) \right\};\ (1 \le u \le X);\ (1 \le h \le Y) \quad (17)$$

Assume that the angles associated with the position, steering, and coordinate of the vehicle of $u^{th}$ rideris $\theta_u$, $N_{u,h}^{\tau}$ and $\delta$. Moreover, the constraints of the vehicle, i.e., brake, gear, and accelerator of $u^{th}$ rideris symbolized as $r_u$, $Q_u$ and $a_u$ correspondingly. The gear $Q_u$ attains a value among 0 and 4, while the brake values $r_u$ and accelerator $a_u$ lie amongst 0 and 1.

**Assessing the achievement rate:** The achievement pace of the rider is refreshed, to such an extent that rider with maximal worth is pronounced as the main rider or best rider, in light of which another rider update themselves. The methodology avoids the nearby assembly, which is the effect of the assailant and on the other hand, the worldwide union is the responsibility of the over taker. At first, the riders experience the irregular instatement effectively to land at the objective. Likewise, the supporter abuses the multidirectional search space inside the pioneer. Moreover, the over taker utilizes the achievement rate and chooses the dimensional space ideally based on directional marker that outfits the enhancement at the terminal assembly point.

**Update the situation of leading rider:** The main rider is foreordained by progress rate or the riders getting the higher achievement rate is said to be pioneer. The main rider is a rider, who is a lot nearer to the objective and it is worth exceptional that the situation of the main rider changes with time contingent upon progress rate. Thus, the achievement pace of the whole riders is processed and the main rider is foreordained at the completion of the cycle.

**Model of the riders' situation:** According to the standard ROA model, there are four sorts of riders: sidestep rider sidesteps the principal way to land at the goal, adherent entices to pursue the pioneer, over taker concerns his own way for landing at the objective, and aggressor lands at the goal by holding the rider's position. Each rider pursues a predefined strategy to land at the objective through the viable administration of the controlling, rigging, brake, and quickening agent of the vehicle. The rider's position is fluctuated by tuning these imperatives following a foreordained methodology and the system is performed till the off-time, $\tau_{off}$ . The detour rider don't pursue the pioneer as the general way is circumvent that is numerically detailed as given by Eq. (18), which is the standard condition of the detour rider in the standard ROA.

$$Z_{u,h}^{\tau+1}(B)=\beta\left\lfloor Z_{\gamma,h}^{\tau}*\alpha(h)+Z_{\eta,h}^{\tau}*(1-\alpha(h))\right\rfloor \quad (18)$$

In Eq. (18), $\beta$ points out an arbitrary number attaining the values among 0 and 1, $\gamma$ refers to the arbitrary number obtaining the values among 1 and $X$ , $\eta$ refer to the arbitrary number lying among 1 and $X$ . Simultaneously, $\chi$ portrays the arbitrary number considering the value among 0 and 1 of size $(1\times Y)$. Therefore, the position of rider is updated at the termination of the individual's iteration to confirm the champion. Concurrently, the follower's position is updated depending on the leader so as to arrive at the target that is designed as shown by Eq. (19). Here, $c$ denotes the coordinate selector, leaders' position be, $Z^{L}$ , $L$ indicates the index of leader, $Z^{L}(L,c)$ , $N_{u,c}^{\tau}$ refers to the steering angle of $u^{th}$ rider in $c^{th}$ coordinate, and $\partial_u^{\tau}$ indicates the distance covered by $u^{th}$ rider.

$$Z_{u,h}^{\tau+1}(F)=Z^{L}(L,c)+\left\lfloor\cos\left(N_{u,c}^{\tau}\right)*Z^{L}(L,c)*\partial_u^{\tau}\right\rfloor \quad (19)$$

In [24], the distance enclosed by the rider is approximated by multiplying $\tau_{off}$ and velocity. The over taker's position will be based on the direction indicator, success rate, and coordinate selector and the corresponding update is specified by Eq. (20). Here, $Z_{u,c}^{\tau}$ denotes the position of $u^{th}$ rider in $c^{th}$ coordinate and $I_u^{\tau}$ indicates the directional indicator of $u^{th}$ rider in $\tau$ and it is computed based on the success rate as given by Eq. (21).

$$Z_{u,c}^{\tau+1}(O)=Z_{u,c}^{\tau}+\left\lfloor I_u^{\tau}*Z^{L}(L,c)\right\rfloor \quad (20)$$

$$I_u^{\tau}=\left\lfloor\frac{2}{1-\log(F_u)}\right\rfloor-1 \quad (21)$$

In Eq. (21), $F_u$ portrays the achievement rate of $u^{th}$ rider at $\tau$ and the higher success rate is observed among $X$ riders, whose value relies among 0 and 1. The assessment of arrange selector is reliant on the variety in the places of driving rider and $u^{th}$ rider. Alternatively, the attacker endeavors to land at the objective after the pioneer with the position update indistinguishable from that of the follower. The assailant's position is given by Eq. (22).

$$Z_{u,h}^{\tau+1}(A)=Z^{L}(L,c)+\left\lfloor\cos\left(N_{u,c}^{\tau}\right)*Z^{L}(L,c)+\partial_u^{\tau}\right\rfloor \quad (22)$$

Activity Counter: It holds a value of 1, if the success rate of rider at time $\tau+1$ goes beyond the rate, which is evaluated at time $\tau$ and 0 is allocated for another case of lagging value as shown in Eq. (23).

$$A_c^{\tau+1}(i)=\begin{cases}1, \text{ if } r_{\tau+1}(i)>r_{\tau}(i)\\ 0, \text{ otherwise}\end{cases} \quad (23)$$

Steering Angle: It is updated depending on the activity counter as shown in Eq. (24).

$$T_{i,j}^{\tau+1}=\begin{cases}T_{i+1,j}^{\tau}, \text{ if } A_c^{\tau+1}(i)=1\\ T_{i-1,j}^{\tau}, \text{ if } A_c^{\tau+1}(i)=1\end{cases} \quad (24)$$

Gear: At $\tau+1$, the vehicle gear is updated based on activity counter, and the higher value of the gear is shown by Eq. (25).

$$E_i^{\tau+1}=\begin{cases}E_i^{\tau}+1, \text{ if } A_c^{\tau+1}(i)=1 \;\&\; E_i^{\tau}\neq|E|\\ E_i^{\tau}-1, \text{ if } A_c^{\tau+1}(i)=0 \;\&\; E_i^{\tau}\neq 0\\ E_i^{\tau}, \quad \text{otherwise}\end{cases} \quad (25)$$

**Rethink the achievement rate:** The rider refreshes the position contingent upon the achievement pace of individual rider and the rider with higher achievement rate go before the race and will be proclaimed as the main rider.

**Update the rider imperatives at the end of the position update:** The rider limitations are refreshed at the end of the emphasis to discover the ideal arrangement. In this way, the requirements to be refreshed comprise of the quickening agent, gear, head out time, brake and controlling point together with the movement counter (incorporates 0 or 1 relying upon progress rate), which is refreshed at the end of the cycle.

**Termination:** The phases of optimization are continued until the termination. At last, the optimal solution is attained by the optimization denoting the particular users. The pseudocode of ROA scheme is highlighted in Algorithm 1.

**Algorithm 1: Conventional ROA Model**

Input: Random positions of riders, $Z_{u,c}^{\tau}$

Output: Leading rider, $Z^{L}$
Assign the population
Assign the rider constraints
Determine the success rate
While, $\tau < \tau_{off}$
for $u = 1$ to $X$
Update bypass position rider as per Eq. (18)
Update follower position as per Eq. (19)
Update over taker position as per Eq. (20)
Update attacker position as per Eq. (22)
Rank riders depending on success rate
Choose rider with higher success rate as leading one.
Update the rider constraints
Return $Z^{L}$
$\tau = \tau + 1$
end for
end while
End

*C. Proposed ISG-ROA Model*

The key factor for each rider to attain the target is not only based on other groups but also the exact handling of steering, gear, accelerator, and brake. In fact, the riders should focus on the target by managing these parameters, and it follows the predefined strategy based on the current success rate. In conventional ROA, activity counter ( $A_c^{\tau+1}(i)$ ) plays a major role in updating the steering angle, and gear. According to the ROA concept, the steering angle is updated if $A_c^{\tau+1}(i) = 1$, and gear is updated if $A_c^{\tau+1}(i) = 0$. In order to further improve the performance of conventional ROA, this paper accomplishes the modification on updating steering angle, and gear with the consideration of both active counter, and best solutions. Here, the distance is measured between each solution with leading solution as per Eq. (26). Further, the solutions are sortedon the basis of minimum distance, and first five solutions are considered as best solutions. The steering angle is updated if it satisfies the condition $A_c^{\tau+1}(i) = 1$, and it belongs to best solutions, and gear is updated if it satisfies the condition $A_c^{\tau+1}(i) = 0$, and it belongs to best solutions. This updating procedure paves the way to improvise the solution at high convergence rate. The pseudocode of proposed ISG-ROA model is highlighted in algorithm 2.

$$Dis = Dis\tan ce(leading\ \ solution, current\ \ solution) \quad (26)$$

**Algorithm 2: Proposed ISG-ROA Model**

Input: Random positions of riders, $Z_{u,c}^{\tau}$

Output: Leading rider, $Z^{L}$
Assign the population
Assign the rider constraints
Determine the success rate
While, $\tau < \tau_{off}$
for $u = 1$ to $X$
If $A_c^{\tau+1}(i) = 1$ and belongs to best solutions
Update steering angle
If $A_c^{\tau+1}(i) = 0$ and belongs to best solutions
Update gear
Update bypass position rider as per Eq. (18)
Update follower position as per Eq. (19)
Update over taker position as per Eq. (20)
Update attacker position as per Eq. (22)
Rank riders depending on success rate
Choose rider with higher success rate as leading one.
Update the rider constraints
Return $Z^{L}$
$\tau = \tau + 1$
end if
end if
end for
end while
End

## VI. RESULTS AND DISCUSSIONS

*A. Simulation procedure*

The proposed medical image compression model using ISG-ROA algorithmhas been implemented in MATLAB 2018a, and the significant results were obtained. The experiment was done for four medical image types namely, CT (image type 1), MRI (image type 2), US (image type 3) and X-ray (image type 4). The database for CT image was obtained from https://isbweb.org/data/vsj/ and https://www.kaggle.com/kmader/siim-medical images/version/6 (Access date: 18-12-2018). The database for MRI image was downloaded from http://prostatemrimagedatabase.com/Database/index.html, and the database for US image was downloaded from https://data.mendeley.com/datasets/wmy84gzngw/1 and http://splab.cz/en/download/databaze/ultrasound. Also, the database for X-ray image was downloaded fromhttps://www.kaggle.com/paultimothymooney/chest-xray-pneumonia. The proposed model was compared with traditional algorithms namely, FF [32], PSO [33], GWO [34], WOA [35] and ROA [24] and accordingly, the CR and statistical analysis were held for four image types.

*B. Analysis on Compression Ratio*

The CR analysis on proposed medical image compression using ISG-ROA model for the four image types is given by Fig. 3. From Fig. 3(a), the best performance of the proposed ISG-ROA scheme for CT image is 2.56% better than FF and on considering the worst performance; the presented scheme is 11.11% superior to FF and 7.5% superior to ROA schemes. Accordingly, from Fig. 3(b), the worst performance of the proposed scheme for MRI image is 2.33% better than FF and 2.33% better than ROA models. In addition, from Fig. 3(c), the worst performance of the adopted ISG-ROA method for US image is 4.44% superior to FF and 2.33% superior to ROA algorithms. Also, the mean performance of the presented scheme is 0.25% better than FF and 0.25% better than ROA schemes. Thus the betterment of the suggested image compression model has been validated by the simulation results.

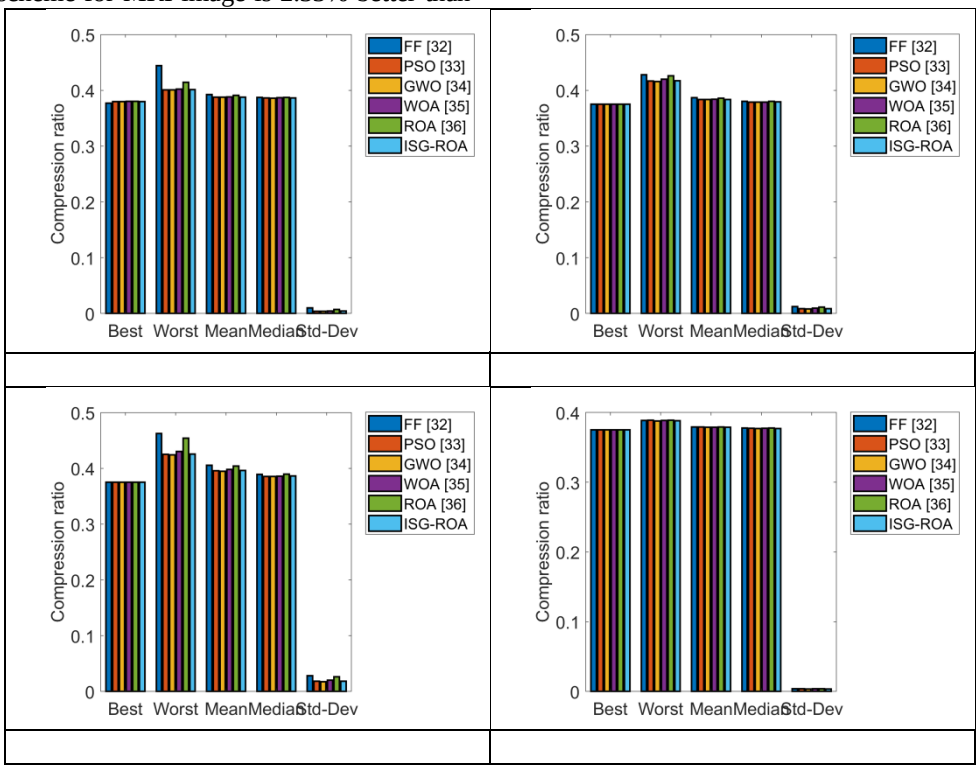


**Fig.3 Analysis on compression ratio for proposed and conventional schemes for (a) CT (b) MRI (c) US (d) XRay**

*C. Error Analysis*

After decompression, the effectiveness of the proposed compression model has been proved by computing the difference between the decompressed and original images in terms of several error measures. Since the entire meta-heuristic algorithms are stochastic in nature, it could not provide optimal outcomes for every execution. Therefore, it is necessary to execute this model for five times and the optimal results are obtained, and best, worst, mean, median and standard deviation is determined. From Table II, the MEP of proposed ISG-ROA scheme in terms of CT image for mean performance is 7.56% better than FF, 8.89% better than PSO, 7.86% better than GWO, 14.15% better than WOA and 6.64% better than ROA schemes. Also, SMAPE of the suggested model is 7.54% superior to FF, 8.57% superior to PSO, 7.68% superior to GWO, 13.79% superior to WOA and 6.45% superior to ROA schemes. In addition, on considering the MASE performance, the developed ISG-ROA model is 1.01% better than FF, 1.23% better than PSO, 1.07% better than GWO, 1.9% better than WOA and 0.64% better than ROA schemes. Moreover, the MAE of proposed scheme in terms of best performance is 5.17% better than FF, 6.58% better than PSO, 4.99% better than GWO, 11.57% better than WOA and 3.83% better than ROA schemes. Moreover, RMSE of the presented ISG-ROA scheme is 4.84% superior to FF, 6.25% superior to PSO, 4.57% superior to GWO, 11.07% superior to WOA and 3.16% superior to ROA schemes in terms of best performance. Also, one norm of the adopted scheme is 0.95% better than FF, 1.17% better than PSO, 1.02% better than GWO, 1.76% better than WOA and 0.53% better than ROA schemes. The two norm of the proposed ISG-ROA scheme in terms of best performance is 4.14% superior to FF, 5.78% superior to PSO, 3.83% superior to GWO, 9.9% superior to WOA and 2.54% superior to ROA schemes. Also, the median performance of the infinity norm is 0.95% better than FF, 1.19% better than PSO, 1.02% better than GWO, 1.77% better than WOA and 0.49% better than ROA schemes. Similarly, the statistical analysis is held for MRI, US and X-Ray as shown in Table III, Table IV and Table V respectively

## VII. CONCLUSION

The paper has presenteda medical image compression model that comprises of three main steps namely, Segmentation, Image compression, and Image decompression. Here, at first, the ROI and Non-ROI portions of the image were divided using MRG algorithm. To the next, the image compression was done which was different

for both Non-ROI and ROI regions. Consequently, the compression process in ROI regions was done by deploying DCT and SPIHT encoding methods, while, the compression of Non-ROI region was made by deploying DWT and MHE approaches. The optimal filter coefficients of DCT, and DWT was obtained by modified algorithm called ISG-ROA. The filter coefficients were adjusted such that the CR should be minimal. Furthermore, decompression was carried out by performing the reverse concept of compression process with same optimized coefficients. From the analysis, the CR in terms of best performance for the proposed scheme for CR image is 2.56% better than FF and on considering the worst performance; the presented scheme was 11.11% superior to FF and 7.5% superior to ROA schemes. Moreover, different error measures were analyzed for validating the decompressed image with compressed image. Thus, the enhancement of the implemented scheme has been confirmed by the simulation outcomes.

## REFERENCES


1. H. Sunil, Sharanabasaweshwar G. Hiremath, "A combined scheme of pixel and block level splitting for medical image compression and reconstruction", Alexandria Engineering Journal, vol. 57, no. 2, pp. 767-772, June 2018.
2. Zhiyong Zuo, Xia Lan, Lihua Deng, Shoukui Yao, Xiaoping Wang, "An improved medical image compression technique with lossless region of interest", Optik - International Journal for Light and Electron Optics, vol. 126, no. 21, pp. 2825-2831, November 2015.
3. Tim Bruylants, Adrian Munteanu, Peter Schelkens, "Wavelet based volumetric medical image compression", Signal Processing: Image Communication, vol. 31, pp. 112-133, February 2015.
4. D. Venugopal, S. Mohan, Sivanantha Raja, "An efficient block based lossless compression of medical images", Optik, vol. 127, no. 2, pp. 754-758, January 2016.
5. S. Haddad, G. Coatrieux, M. Cozic, D. Bouslimi, "Joint Watermarking and Lossless JPEG-LS Compression for Medical Image Security", IRBM, vol. 38, no. 4, pp. 198-206, August 2017.
6. X. Song, Q. Huang, S. Chang, J. He and H. Wang, "Three-dimensional separate descendant-based SPIHT algorithm for fast compression of high-resolution medical image sequences," IET Image Processing, vol. 11, no. 1, pp. 80-87, 1 2017.
7. S. S. Parikh, D. Ruiz, H. Kalva, G. Fernández-Escribano and V. Adzic, "High Bit-Depth Medical Image Compression With HEVC," IEEE Journal of Biomedical and Health Informatics, vol. 22, no. 2, pp. 552-560, March 2018.
8. L. F. R. Lucas, N. M. M. Rodrigues, L. A. da Silva Cruz and S. M. M. de Faria, "Lossless Compression of Medical Images Using 3-D Predictors," IEEE Transactions on Medical Imaging, vol. 36, no. 11, pp. 2250-2260, Nov. 2017.
9. A. J. Hussain, Ali Al-Fayadh, Naeem Radi, "Image compression techniques: A survey in lossless and lossy algorithms", Neurocomputing, vol. 300, pp. 44-69, 26 July 2018.
10. Xie Kai, Yang Jie, Zhu Yue Min, Li Xiao Liang, "HVS-based medical image compression", European Journal of Radiology, vol. 55, no. 1, pp. 139-145, July 2005.
11. Anke Meyer-Bäse, Karsten Jancke, Axel Wismüller, Simon Foo, Thomas Martinetz, "Medical image compression using topology-preserving neural networks", Engineering Applications of Artificial Intelligence, vol. 18, no. 4, pp. 383-392, June 2005.
12. Med Karim Abdmouleh, Ali Khalfallah, Med Salim Bouhlel, "A Novel Selective Encryption Scheme for Medical Images Transmission based-on JPEG Compression Algorithm", Procedia Computer Science, vol. 112, pp. 369-376, 2017.
13. Sujitha Juliet Devaraj, Kirubakaran Ezra, A. Allvin, "3-D Medical Image Compression for Telemedicine Application", Procedia Engineering, vol. 38, pp. 1444-1449, 2012.
14. M. Khalid Khan Niazi, Y. Lin, F. Liu, A. Ashok, A. Bilgin, "Pathological image compression for big data image analysis: Application to hotspot detection in breast cancer", Artificial Intelligence in Medicine, 25 September 2018.
15. Corinne Balleyguier, Morgane Cousin, Ariane Dunant, Marie Attard, Julia Arfi-Rouche, "Patient-assisted compression helps for image quality reduction dose and improves patient experience in mammography", European Journal of Cancer, vol. 103, pp. 137-142, November 2018.
16. N. Sriraam, R. Shyamsunder, "3-D medical image compression using 3-D wavelet coders", Digital Signal Processing, vol. 21, no. 1, pp. 100-109, January 2011.
17. Seyed Morteza Hosseini, Ahmad-Reza Naghsh-Nilchi, "Medical ultrasound image compression using contextual vector quantization", Computers in Biology and Medicine, vol. 42, no. 7, pp. 743-750, July 2012.
18. Sukhwinder Singh, Vinod Kumar, H. K. Verma,"Adaptive threshold-based block classification in medical image compression for teleradiology", Computers in Biology and Medicine, vol. 37, no. 6, pp. 811-819, June 2007.
19. Yao-Tien Chen, Din-Chang Tseng, "Wavelet-based medical image compression with adaptive prediction" ,Computerized Medical Imaging and Graphics, vol. 31, no. 1, pp. 1-8, January 2007.
20. Giuseppe Placidi, "Adaptive compression algorithm from projections: Application on medical greyscale images", Computers in Biology and Medicine, vol. 39, no. 11, pp. 993-999, November 2009.
21. M. A. Ansari, R. S. Anand, " Context based medical image compression for ultrasound images with contextual set partitioning in hierarchical trees algorithm", Advances in Engineering Software, vol. 40, no. 7, pp. 487-496, July 2009.
22. Chenyi Zhao, Zeqi Wang, Huanyu Li, Xiaoyang Wu, Jianing Sun, "A new approach for medical image enhancement based on luminance-level modulation and gradient modulation", Biomedical Signal Processing and Control, vol. 48, pp. 189-196, February 2019.
23. Richa Gupta, Deepti Mehrotra, Rajesh Kumar Tyagi, "Comparative analysis of edge-based fractal image compression using nearest neighbor technique in various frequency domains", Alexandria Engineering Journal, vol. 57, no. 3, pp. 1525-1533, September 2018.
24. D. Binu and B. S. Kariyappa, "RideNN: A New Rider Optimization Algorithm-Based Neural Network for Fault Diagnosis in Analog Circuits," IEEE Transactions on Instrumentation and Measurement.
25. G. Pajares, J.M. de la Cruz, "A wavelet-based image fusion tutorial", Pattern Recognition, vol. 37, no.9, pp. 1855–1872, 2004.
26. H. Li, B.S. Manjunath, S.K. Mitra, "Multisensor image fusion using the wavelet transform", Graphical Models and Image Processing, vol.57, no.3, pp. 235–245, 1995.
27. I. De, B. Chanda, "A simple and efficient algorithm for multifocus image fusion using morphological wavelets", Signal Processing, vol. 86 no.5,pp.924–936, 2006.
28. G.Ramesh Babu and K.Veera Swamy, "Image Fusion using various Transforms", IPASJ International Journal of Computer Science (IIJCS), vol.2, no.1, January 2014.
29. Xin Jin, Qian Jiang, Shaowen Yao, Dongming Zhou, Kangjian He, ":Infrared and visual image fusion method based on discrete cosine transform and local spatial frequency in discrete stationary wavelet transform domain", Infrared Physics & Technology, vol. 88, pp. 1-12, January 2018.
30. Shuyuan Yang, RuiXia Wu, Min Wang, Licheng Jiao, "Evolutionary clustering based vector quantization and SPIHT coding for image compression", Pattern Recognition Letters, vol. 31, no. 13, pp. 1773-1780, 1 October 2010.
31. M. M. Almi'ani and B. D. Barkana, "A modified region growing based algorithm to vessel segmentation in magnetic resonance angiography," 2015 Long Island Systems, Applications and Technology, Farmingdale, NY, pp. 1-7, 2015.
32. Iztok Fister, Iztok Fister, Xin-She Yang, Janez Brest, "A comprehensive review of firefly algorithms", Swarm and Evolutionary Computation, vol. 13, pp. 34-46, December 2013.
33. Junhao Zhang, Pinqi Xia, "An improved PSO algorithm for parameter identification of nonlinear dynamic hysteretic models", Journal of Sound and Vibration, vol. 389, pp. 153-167, 17 February 2017.
34. Seyedali Mirjalili a, Seyed Mohammad Mirjalili, Andrew Lewis, "Grey Wolf Optimizer", Advances in Engineering Software, vol. 69, pp.46–61, 2014.
35. SeyedaliMirjalili, Andrew Lewis, "The Whale Optimization Algorithm", Advances in Engineering Software, vol. 95, pp. 51-67, May 2016.

## AUTHOR PROFILE

**Mr.P.Sreenivasulu** obtained his Bachelor's degree in Electronics and Communication Engineering from S.V University,Tirupathi and his Master's degree in Electronics Instrumentation and communication systems. Currently he is pursuing PhD in Digital Image processing from S.V University, Tirupathi, Andhra Pradesh. At present, he is working as **Associate Professor in the department of** Electronics And Communication Engineering at Audisankara College of Engineering and Technology,Gudur,A.P. He has published 10 Papers in International Journals and 5 papers in National Journals. He has Total Teaching Experience of 13 years.

Dr.S.Varadarajan has received his PhD from S V University. He hasmore than 25 years of teaching experience. He is working as a Professor in the department of ECE in S V University. He is published more than 100 papers in various reputed journals and presented 65 papers in national and international conferences. He is in an active member of various professional bodies.

Dr.S.Thenappan has received his PhD from JNTU Anantapur. He has more than 20 years of teaching experience. He is working as a Professor in the department of ECE in KNS Institute of Technology, Bangalore.